

Synthesis and characterization of an unusual lamellar aluminophosphate synthesized from an alcohol system†

Qiuming Gao,^a Ruren Xu,^{*a} Jiasheng Chen,^a Rongsheng Li,^a Shougui Li,^a Shilun Qiu^a and Yong Yue^b

^a Key Laboratory of Inorganic Hydrothermal Synthesis, Department of Chemistry, Jilin University, Changchun 130023, China

^b Wuhan Institute of Physics, Academia Sinica, Wuhan 430071, China

An unusual lamellar aluminophosphate $[Al_4P_2O_{11} \cdot 2C_6H_{13}NH_2 \cdot 4H_2O] \cdot 3H_2O$ was synthesized from a mixture of H_3PO_4 , $Al(OPr^i)_3$, ethylene glycol and an unbranched primary alcohol. It was characterized by X-ray powder diffraction, scanning electron microscopy, infrared, magic angle spinning NMR spectroscopy, differential thermal and thermogravimetric analysis. It is composed of PO_4 , AlO_4 and AlO_6 structural units, and the ratio of octahedral to tetrahedral Al in the as-synthesized compound is about 1:1. This material exhibits a very large weight loss at elevated temperatures. Upon dehydration it possesses a considerable water adsorption capacity. The water adsorption isotherm is linear. Of the seven water molecules in the empirical formula, four are co-ordinated to the Al atoms and the other three are located between adjacent layers.

During the past two decades considerable research activity has been devoted to metal phosphates and phosphonates with low dimensionalities (one-dimensional chain and two-dimensional lamellar structures) as they are potentially applicable in the areas of catalysis, ion exchange, molecular recognition, optics and electronics.¹⁻⁴ A number of lamellar metal phosphates and phosphonates have been discovered,⁵⁻¹³ and those falling into the category of mesophases have an interlamellar distance of 20–100 Å. Among them are the molecule-intercalated inorganic phosphates and metal phosphonate multilayer films. The former possess inorganic layers with organic molecules sandwiched between the adjacent layers whereas in the latter the organic groups are chemically bonded to the phosphorus atoms. Organic groups can also be bonded to the O atoms of the phosphate anions which comprise the inorganic layers with metal cations. Whereas layered phosphates and phosphonates of di- and tetra-valent metals having a large interlamellar distance have frequently been encountered, lamellar mesophases of trivalent-metal phosphates or phosphonates are rare. The interlamellar distance of the layered aluminophosphates reported previously¹⁰⁻¹⁵ is invariably less than 15 Å, and although their structures and compositions can be varied to a great extent, few exhibit significant water adsorption capacities since the layers are either hydrophobic or lack void spaces to accommodate guest molecules. Very recently Ozin and co-workers¹⁶ described the synthesis of a mesolamellar aluminophosphate from an alcoholic system using tetraethylene glycol $[O(CH_2CH_2OCH_2CH_2OH)_2]$ as the solvent. This lamellar material has a *d* spacing of 29.42 Å and an Al:P ratio of 1:2. In this paper, we describe the synthesis and characterization of a lamellar aluminophosphate mesophase having an Al:P ratio of 2:1, *i.e.* the inorganic layer for the materials is a basic aluminophosphate. It contains a large amount of water and upon dehydration at 100 °C under vacuum it exhibits a considerable water adsorption capacity. The water adsorption isotherm is linear, being different from the five conventional types of physical adsorption isotherms.

Experimental

The compound was synthesized from a predominantly non-aqueous system in which a mixture of ethylene glycol ($HOCH_2-CH_2OH$) and an unbranched primary alcohol ($n-C_nH_{2n+1}OH$, $n = 4-8$) was used as the medium and hexylamine as the template. Thus, aluminium triisopropoxide, phosphoric acid (85%) and hexylamine were successively added to the medium. After stirring for a few hours a gel with an empirical molar composition of $Al(OPr^i)_3 : 1.8H_3PO_4 : 3.4n-C_6H_{13}NH_2 : 3.4n-C_nH_{2n+1}OH : 13.8HOCH_2CH_2OH : 1.7H_2O$ was formed. It was sealed in a Teflon-lined stainless autoclave and heated under autogenous pressure at 180 °C for 8 d. The crystalline product was filtered off, washed with water and dried at ambient temperature.

Element analysis was performed on a Perkin-Elmer 240C element analyser. X-Ray powder diffraction (XRD) data were collected on a Rigaku D/MAX III A diffractometer with nickel-filtered $Cu-K\alpha$ radiation ($\lambda = 1.5418 \text{ \AA}$). The sample was scanned from 2.5 to 40° (2 θ) at a scan speed of 1° min⁻¹. Scanning electron micrographs were taken on a Hitachi X-650 electron microscope. The infrared spectrum was recorded on a Nicolet 5DX FTIR spectrometer using KBr pellets. A Perkin-Elmer DTA 1700 differential thermal analyser was used to conduct the differential thermal analysis (DTA) and a Perkin-Elmer TGA 7 thermogravimetric analyser to obtain the thermogravimetric analysis (TGA) curves in a nitrogen atmosphere. The temperature was increased at 20 °C min⁻¹ and the flow of N_2 was 50 cm³ min⁻¹. Adsorption measurements were conducted on a Cahn 2000 vacuum electrobalance system.

The magic angle spinning (MAS) ²⁷Al NMR spectra were recorded on a Bruker MSL-400 spectrometer with a magnetic field strength of 9.4 T and spinning rates of 10 kHz. The single-pulse excitation technique was applied and the spectra were obtained at 104.3 MHz. Other parameters: pulse width, 0.5 μ s; recycle delay, 10 s; number of transients, 1000. The chemical shifts were relative to aqueous $Al(NO_3)_3$ as external standard. The MAS ¹³C and ³¹P NMR spectra were obtained on a Bruker MSL-400 spectrometer (9.4T) with spinning rates of 5 and 6 kHz, respectively. The cross-polarization technique was applied. The contact time was 5.0 ms and the scan number 1000 with a recycle delay of 14 s. The chemical shifts were relative to $SiMe_4$ and H_3PO_4 (85% w/w), respectively.

† Non-SI units employed: Torr \approx 133 Pa, atm = 101 325 Pa.

Results and Discussion

Formation and composition

The use of a mixed solvent is very important for the synthesis. If ethylene glycol and unbranched primary alcohols are used independently as the solvent, the compound is not obtained. On the other hand, it seems that the polarity of the co-solvent (unbranched primary alcohol) also plays an important role as suggested by the fact that the compound forms readily in the presence of both ethylene glycol and a larger unbranched primary alcohol such as butanol, pentanol, hexanol, heptanol or octanol, whereas only an amorphous phase exists when a shorter unbranched primary alcohol (methanol, ethanol or propanol) is used.

The preferred source of phosphorus is orthophosphoric acid which has a good solubility in alcoholic solvents. In an alcoholic medium, an ester of phosphoric acid does not react with aluminium triisopropoxide and inorganic phosphates are difficult to dissolve, therefore they are not suitable phosphorus sources. The most reactive source of aluminium is $\text{Al}(\text{OPr}^i)_3$ and the Pr^iOH evolved from it does not affect the nature of the alcoholic medium. Pseudoboehmite, an excellent aluminium source for the preparation of microporous aluminophosphates in aqueous media, and other inorganic aluminium sources such as aluminium sulfate and sodium aluminate, has a very low solubility in the alcohol systems.

The crystallization temperature is also an important factor for the synthesis. A temperature of 200 °C or above results in a large amount of AlPO_4 tridymite in the product without the appearance of the required phase; whereas at < 160 °C only an amorphous material is formed.

The chemical analysis indicated a P:Al ratio of 0.5:1 and the element analysis revealed that the N, C, H contents are 4.30, 21.45 and 6.05%, respectively, corresponding to a molar ratio N:C:H = 0.17:1.00:3.39. The empirical composition calculated on the basis of the analysis data is $2.0\text{Al}_2\text{O}_3 \cdot 1.1\text{P}_2\text{O}_5 \cdot 2.1\text{C}_6\text{H}_{13}\text{NH}_2 \cdot 7.2\text{H}_2\text{O}$, which can be normalized to $\text{Al}_4\text{P}_2\text{O}_{11} \cdot 2\text{C}_6\text{H}_{13}\text{NH}_2 \cdot 7\text{H}_2\text{O}$. It is interesting that the Al:P ratio is 2:1, in contrast with those for previously reported aluminophosphates synthesized from alcoholic systems which invariably have a P:Al ratio greater than 1:1. Aluminophosphates with Al:P ratio greater than unity fall into the basic category, and are represented by a series of minerals.¹⁷

X-Ray powder diffraction and scanning electron microscopy

The X-ray powder diffraction pattern (Fig. 1) shows only three peaks, with d spacings of 22.50, 11.23 and 7.50 Å, respectively. As for the lamellar silicate mesophase^{9,18,19}, these peaks are attributable to the (001), (002) and (003) reflections, showing that the compound has a lamellar structure, with an interlamellar distance of ca. 22.5 Å. Using *n*-octyl-, *n*-decyl- or *n*-dodecyl-amine as the template, three aluminophosphates have been synthesized, the XRD patterns of which also show only three peaks, which can be attributable to the (001), (002) and (003) reflections, with d_{001} = 26.53, 30.68 and 34.70 Å, respectively. They further reveal that the structure of this family is lamellar. The interlamellar distance is shorter than that (ca. 40 Å) of the surfactant-containing lamellar silicate^{18,19} owing to the length of the unbranched fatty chain of the template being shorter than that of the surfactant in the lamellar silicate. However, it must be emphasized that this interlamellar distance is similar to that for the mesolamellar aluminophosphate material,¹⁶ but considerably greater than those (ca. 10 Å) of lamellar aluminophosphates¹⁰⁻¹⁴ reported previously, where the templates used were short-chain amines.

A scanning electron micrograph (Fig. 2) shows that the crystals appear as thin plates with diameters of 10–20 µm, characteristic of layered materials. The shape of the plate is irregular, different from that of the known lamellar

aluminophosphates which normally exhibit well defined three-dimensional morphologies.

Infrared spectrum

Fig. 3 shows the infrared spectrum in the region 4000–400 cm^{-1} . On the basis of the framework vibration model for microporous aluminophosphates,²⁰⁻²³ the absorption bands are assigned as follows: 1075 cm^{-1} , asymmetric stretching of Al–O–P; 794 and 730 cm^{-1} , symmetric stretching of Al–O–P; 534 cm^{-1} , skeletal bend of Al–O–P. Bands due to the template $n\text{-C}_6\text{H}_{13}\text{NH}_2$ ²⁴ are also observed: 1546 cm^{-1} , bending $\delta(\text{N-H})$ of NH_2 ; 1469 and 1384 cm^{-1} , bending $\delta(\text{C-H})$ of CH_3 ; 2965 and 2931 cm^{-1} , asymmetric stretching of CH_3 or CH_2 ; 2861 cm^{-1} , symmetric stretching of CH_3 or CH_2 . The spectrum also exhibits an absorption around 1638 cm^{-1} , revealing the presence of water molecules.

MAS NMR spectra

In the MAS ³¹P NMR spectra of the mixed reaction gel (Fig. 4) only one peak at δ –8.2 is observed, suggesting the presence of phosphorus atoms in a reasonably uniform tetrahedral coordination environment.²⁵⁻²⁷ The ³¹P NMR spectrum of the

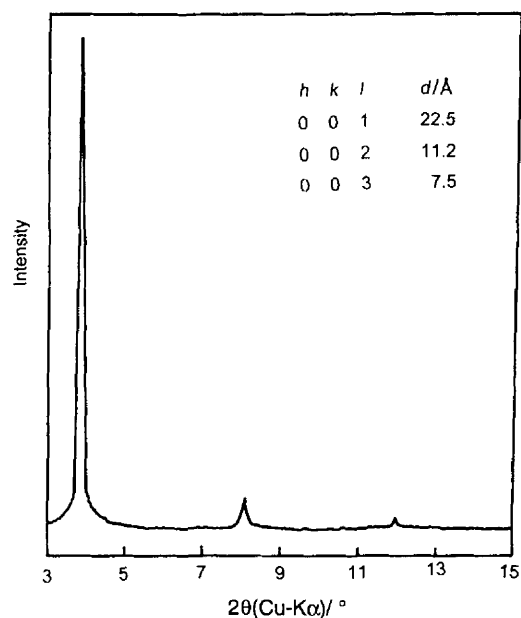


Fig. 1 X-Ray powder diffraction pattern for $\text{Al}_4\text{P}_2\text{O}_{11} \cdot 2\text{C}_6\text{H}_{13}\text{NH}_2 \cdot 7\text{H}_2\text{O}$

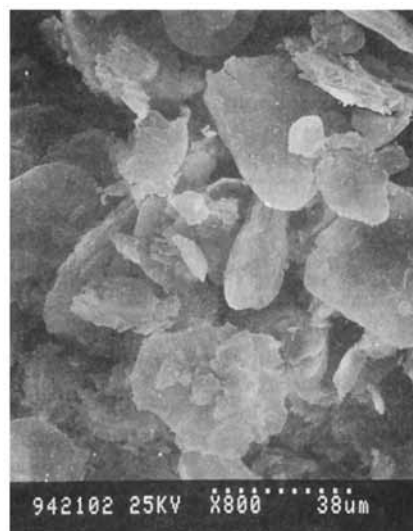


Fig. 2 Scanning electron micrograph of crystals of $\text{Al}_4\text{P}_2\text{O}_{11} \cdot 2\text{C}_6\text{H}_{13}\text{NH}_2 \cdot 7\text{H}_2\text{O}$

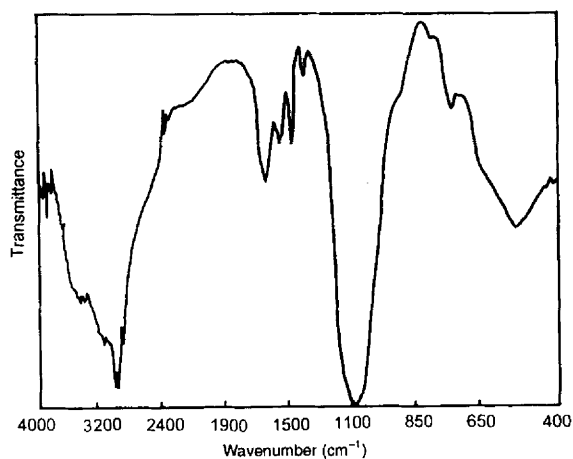


Fig. 3 The IR spectrum in the region 4000–400 cm^{-1}

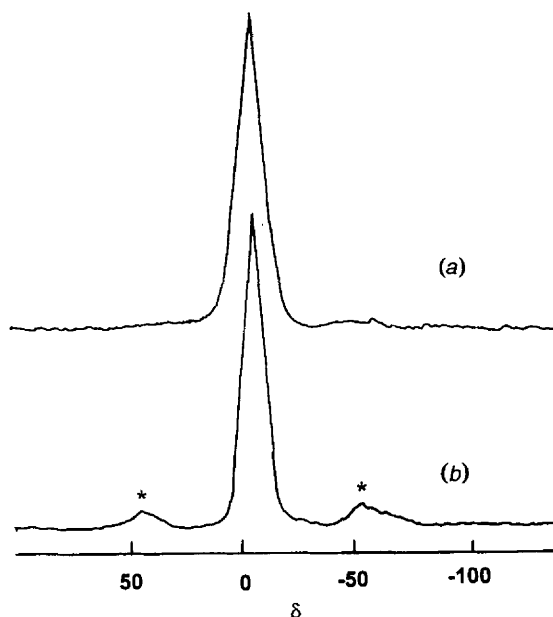


Fig. 4 The MAS ^{31}P NMR spectra of (a) the reaction gel and (b) $\text{Al}_4\text{P}_2\text{O}_{11}\cdot 2\text{C}_6\text{H}_{13}\text{NH}_2\cdot 7\text{H}_2\text{O}$. The asterisks represent sidebands

aluminophosphate also exhibits one peak but the maximum shifts slightly to $\delta -7.8$. The similarity between these two spectra indicates that the local environment of the P atoms remains more or less the same when the gel is transformed into the aluminophosphate.

The MAS ^{27}Al NMR spectrum of the gel (Fig. 5) exhibits one signal at $\delta 4.3$, characteristic of aluminium atoms octahedrally co-ordinated by O atoms.^{25–27} The ligands for the Al are probably water molecules. The corresponding spectrum of the aluminophosphate shows a peak centred at $\delta 45.4$, attributable to Al in tetrahedral symmetry, and another at $\delta -8.1$ assigned to Al in octahedral symmetry. It is interesting that the areas of the two peaks are more or less equal [Fig. 5(a)], suggesting that the molar ratio of octahedral to tetrahedral Al is *ca.* 1:1.

Five peaks appear in the MAS ^{13}C NMR spectrum (Fig. 6) of the aluminophosphate at $\delta 14.2, 23.4, 27.8, 32.2$ and 40.0 , respectively, with the ratio of the peak areas $\alpha:\beta:\gamma:\delta:\eta = 1:1:2:1:1$,²⁸ corresponding to the five different types of carbons in the template molecule $\text{NH}_2\text{C}_\alpha\text{H}_2\text{C}_\beta\text{H}_2\text{C}_\gamma\text{H}_2\text{C}_\delta\text{H}_2\text{C}_\eta\text{H}_3$. This also suggests that $n\text{-C}_6\text{H}_{13}\text{NH}_2$ is essentially intact in the compound.

Thermal properties

Thermogravimetric analysis (Fig. 7) indicates that there is a weight loss of 23.2% from 100 to 180 $^\circ\text{C}$ and one of 29.1% from

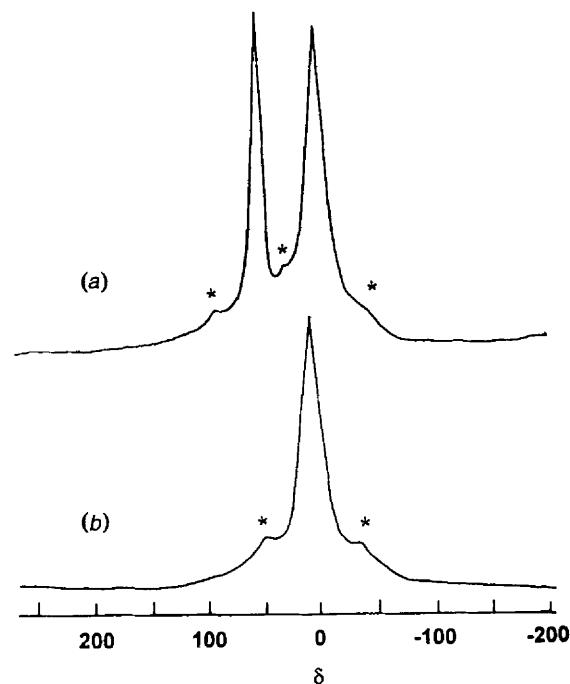


Fig. 5 The MAS ^{27}Al NMR spectra of (a) the reaction gel and (b) $\text{Al}_4\text{P}_2\text{O}_{11}\cdot 2\text{C}_6\text{H}_{13}\text{NH}_2\cdot 7\text{H}_2\text{O}$

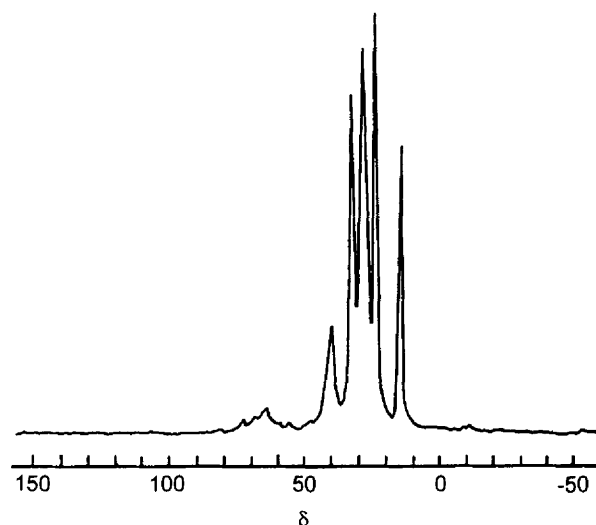


Fig. 6 The MAS ^{13}C NMR spectrum of $\text{Al}_4\text{P}_2\text{O}_{11}\cdot 2\text{C}_6\text{H}_{13}\text{NH}_2\cdot 7\text{H}_2\text{O}$

180 to 430 $^\circ\text{C}$. The first weight loss is associated with the removal of water and the second to decomposition of the template $n\text{-C}_6\text{H}_{13}\text{NH}_2$. Correspondingly, two endothermic peaks at 113 and 264 $^\circ\text{C}$ are observed in the DTA curves. The temperature for desorption of water is marginally higher than that of the boiling point of water, indicating that the interaction between the water molecules and the aluminophosphate layers is not very strong. The decomposition temperature of the template $n\text{-C}_6\text{H}_{13}\text{NH}_2$ is high enough for the material to withstand removal of the water molecules without destruction of its structure. The total weight loss is about 52.3%, much larger than that (less than 40%) for other known lamellar aluminophosphates containing a template and for the as-synthesized aluminophosphate molecular sieves, such as $\text{AlPO}_4\text{-41}$ ²⁹ with a one-dimensional medium-pore framework, $\text{AlPO}_4\text{-17}$ ³⁰ with a cage-containing framework and JDF-20 $\{[\text{Al}_5\text{P}_6\text{O}_{24}\text{H}]^{2-} \cdot 2[\text{N}(\text{C}_5\text{H}_5)_3\text{H}]^+ \cdot 2\text{H}_2\text{O}\}$,^{31,32} an aluminophosphate possessing 20-membered ring channels. X-Ray powder diffraction at different temperature shows that the present aluminophosphate is stable when calcined below 420 $^\circ\text{C}$ and no phase transformation occurs. However, with an increase

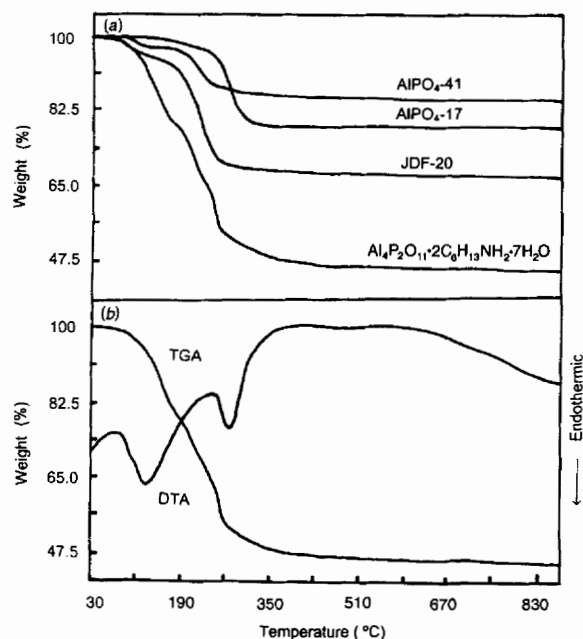


Fig. 7 (a) The TGA curves for AlPO_4 -41, AlPO_4 -17, JDF-20 and $\text{Al}_4\text{P}_2\text{O}_{11}\cdot 2\text{C}_6\text{H}_{13}\text{NH}_2\cdot 7\text{H}_2\text{O}$ and (b) the TGA and DTA curves for $\text{Al}_4\text{P}_2\text{O}_{11}\cdot 2\text{C}_6\text{H}_{13}\text{NH}_2\cdot 7\text{H}_2\text{O}$

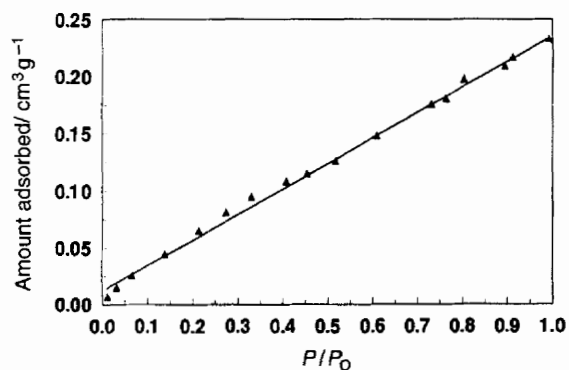


Fig. 8 Adsorption isotherm of water at 293 K

in calcination temperature the crystallinity of the sample apparently decreases. When the temperature reaches 350 °C, the material changes from crystalline to amorphous form. With increasing calcination temperature a series of phase transitions take place. The XRD analysis of the thermal transformation sequences indicate the behaviour to be consistent with the transitions: < 320 °C, $\text{Al}_4\text{P}_2\text{O}_{11}\cdot 2\text{C}_6\text{H}_{13}\text{NH}_2\cdot 7\text{H}_2\text{O}$; 350–400 °C, AlPO_4 tridymite (mixed with amorphous); 450–850 °C, AlPO_4 tridymite and γ -alumina; 1000 °C, AlPO_4 tridymite, δ - and θ -alumina; 1100 °C, AlPO_4 tridymite, δ -, θ - and α -alumina.

Isothermal adsorption of water

The water-adsorption isotherm at 293 K for the aluminophosphate is shown in Fig. 8. Prior to the measurement the sample was dehydrated at 373 K and 10^{-3} Torr. The isotherm is linear within the experimental relative pressure range. In other words, the adsorption equilibrium of water on the sample can be described by Henry's law over quite a wide range of relative pressure. The isotherms at 273 and 323 K were also measured, and the amounts of water adsorbed are also linearly proportional to the vapour pressure (see Fig. 9). Henry's constants can be calculated from Fig. 9 and are expressed as³³ in equation (1) where Q is the amount adsorbed in $\text{cm}^3 \text{g}^{-1}$ and

$$Q/Q^0 = K_h P \quad (1)$$

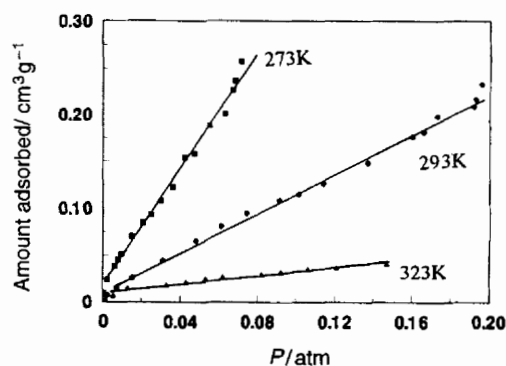


Fig. 9 Amount of water adsorbed versus vapour pressure at 273, 293 and 323 K

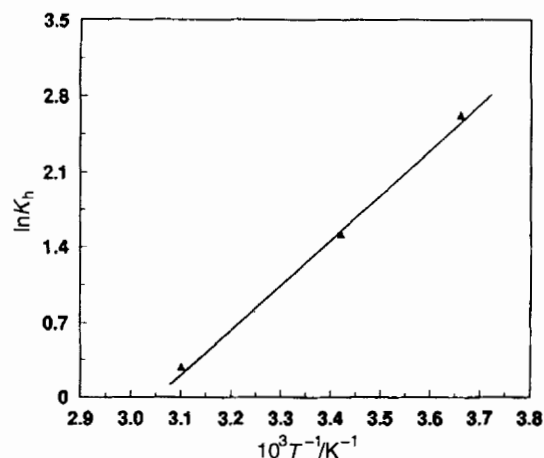


Fig. 10 Plot of $\ln K_h$ against $1/T$ for water adsorption on $\text{Al}_4\text{P}_2\text{O}_{11}\cdot 2\text{C}_6\text{H}_{13}\text{NH}_2\cdot 7\text{H}_2\text{O}$

Q^0 is the equilibrium adsorption capacity assumed equal to the amount of water adsorbed ($0.232 \text{ cm}^3 \text{ g}^{-1}$)* at 393 K and $P/P_0 = 1.0$. A standard state of 1 atm is also assumed. To a first approximation, the adsorption enthalpy ΔH and the adsorption entropy ΔS are independent of temperature within the experimental temperature region, and can be evaluated from equation³⁴ (2). The ΔH° and ΔS° values obtained from a plot

$$\ln K_h = -(\Delta H^\circ/RT) + (\Delta S^\circ/R) \quad (2)$$

(Fig. 10) of $\ln K_h$ against $1/T$ are presented in Table 1. The adsorption free energy ΔG° was calculated from equation (3)

$$\Delta G^\circ = -RT \ln K_h \quad (3)$$

and the values at the three temperatures are also listed in Table 1.

The adsorption enthalpy ($-36.88 \text{ kJ mol}^{-1}$)† indicates that the interaction between the adsorbed water molecules and the framework atoms of the host material is not very strong. The XRD and MAS ^{31}P NMR data for the sample with adsorbed water are basically the same as those for the sample without this water, showing that the layered structure of the compound is not destructively affected by adsorption-desorption, and also that the template is not desorbed since the d_{001} value is basically not changed, in accord with the TGA-DTA results. The

* This result comes from the largest experimental value, at 393 K and $P/P_0 = ca. 1$, from the equation % adsorbed water = V/M where V is the volume of adsorbed water and M the mass of $\text{Al}_4\text{P}_2\text{O}_{11}\cdot 2\text{C}_6\text{H}_{13}\text{NH}_2$, not including co-ordinated and interlamellar water.

† It cannot be considered to be the co-ordination reaction enthalpy because the adsorption occurs in two steps, co-ordination between the water molecules and Al and entry of the water molecules into the interlamellar space. These two steps cannot be resolved.

Table 1 Thermodynamic data for water adsorption on $\text{Al}_4\text{P}_2\text{O}_{11}\cdot 2\text{C}_6\text{H}_{13}\text{NH}_2$

T/K	K_h	$\Delta G^\circ_T/\text{kJ mol}^{-1}$
273	13.78	-5.95
293	4.55	-3.68
323	1.33	-0.33

$$\Delta H^\circ = -36.88 \text{ kJ mol}^{-1}, \Delta S^\circ = -113.4 \text{ J K}^{-1} \text{ mol}^{-1}.$$

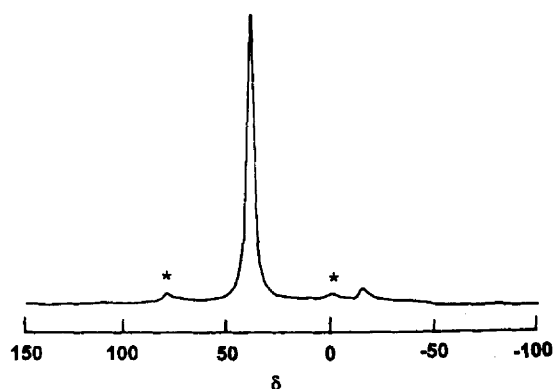


Fig. 11 The MAS ^{27}Al NMR spectrum of $\text{Al}_4\text{P}_2\text{O}_{11}\cdot 2\text{C}_6\text{H}_{13}\text{NH}_2\cdot 7\text{H}_2\text{O}$ after dehydration at 373 K and 10^{-3} Torr for 2 h

adsorption entropy ($113.4 \text{ J K}^{-1} \text{ mol}^{-1}$) is similar to those for the adsorption of molecules on microporous materials,³³ suggesting that the entropy contribution to the adsorption free energy of water in the aluminophosphate is similar to that for microporous packing of guest molecules.

Nature of adsorbed water

The MAS ^{27}Al NMR spectrum (Fig. 11) of the aluminophosphate dehydrated at 373 K and 10^{-3} Torr shows a strong signal at δ 38.9 and a very weak one at δ -15.0. The former is attributable to tetrahedral Al, the latter to octahedral Al. This implies that almost all the Al atoms in the dehydrated material are in tetrahedral symmetry. Obviously, the six-co-ordinated Al atoms in the as-synthesized aluminophosphate are transformed into four-co-ordinated ones after dehydration. The presence of the former atoms must be due to the adsorbed water co-ordinating as extra ligands. This is in sharp contrast with the lack of co-ordinated water in previously reported layered aluminophosphates with smaller interlamellar distances.¹⁰⁻¹⁴ These layered aluminophosphates contain only four-co-ordinated Al atoms. On the other hand, the presence of six-co-ordinated Al atoms is very common³⁵⁻³⁷ for hydrated-detemplated aluminophosphate molecular sieves. It seems that the water adsorption behaviour of the present aluminophosphate is similar to that of microporous aluminophosphate molecular sieves rather than to that of layered aluminophosphates with small intercalated molecules.

Assuming that each six-co-ordinated Al in the as-synthesized $\text{Al}_4\text{P}_2\text{O}_{11}\cdot 2\text{C}_6\text{H}_{13}\text{NH}_2\cdot 7\text{H}_2\text{O}$ is bound to two extra water ligands, the fact that the octahedral:tetrahedral aluminium ratio is about 1:1 on the basis of the NMR signals suggest that four of the seven water molecules in the composition are co-ordinated to two Al atoms, and the other three are accommodated somewhere between the layers. Therefore, it is more appropriate for the formula to be written as $[\text{Al}_4\text{P}_2\text{O}_{11}\cdot 2\text{C}_6\text{H}_{13}\text{NH}_2\cdot 4\text{H}_2\text{O}]\cdot 3\text{H}_2\text{O}$.

Acknowledgements

We are grateful to the National Natural Science Foundation of China and the Ph.D. Studentship Foundation of the State Education Commission of China for financial support.

References

- 1 T. Kanazawa, *Inorganic Phosphate Materials*, Elsevier, Tokyo, 1989.
- 2 R. H. Jones, J. M. Thomas, R. Xu, Q. Huo, Y. Xu, A. K. Cheetham and D. Bieber, *J. Chem. Soc., Chem. Commun.*, 1990, 1170.
- 3 G. Cao, H. Hong and T. E. Mallouk, *Acc. Chem. Res.*, 1992, **25**, 420.
- 4 G. A. Ozin, *Adv. Mater.*, 1992, **4**, 612.
- 5 A. Clearfield, *Chem. Rev.*, 1988, **88**, 125.
- 6 J. Chen, S. Natarajan, P. A. Wright, R. H. Jones, J. M. Thomas and C. R. A. Catlow, *J. Solid State Chem.*, 1993, **103**, 519.
- 7 G. Cao, V. M. Lynch and J. N. Yacullo, *Chem. Mater.*, 1993, **5**, 1000.
- 8 M. I. Khan, Y. S. Lee, C. J. O'Connor, R. C. Haushalter and J. Zubieta, *J. Am. Chem. Soc.*, 1994, **116**, 4525.
- 9 Q. Huo, D. I. Margolese, U. Ciesla, D. G. Demuth, P. Feng, T. E. Gier, P. Sieger, A. Firouzi, B. F. Chmelka, F. Schuth and G. D. Stucky, *Chem. Mater.*, 1994, **6**, 1176.
- 10 R. H. Jones, J. M. Thomas, R. Xu, Q. Huo, A. K. Cheetham and A. V. Powell, *J. Chem. Soc., Chem. Commun.*, 1991, 1266.
- 11 A. M. Chippindale, A. V. Powell, L. M. Bull, R. H. Jones, A. K. Cheetham, J. M. Thomas and R. Xu, *J. Solid State Chem.*, 1992, **96**, 199.
- 12 J. M. Thomas, R. H. Jones, R. Xu, J. Chen, A. M. Chippindale, S. Natarajan and A. K. Cheetham, *J. Chem. Soc., Chem. Commun.*, 1992, 929.
- 13 A. M. Chippindale, S. Natarajan, J. M. Thomas and R. H. Jones, *J. Solid State Chem.*, 1994, **111**, 18.
- 14 D. Riou, Th. Loiseau and G. Ferey, *J. Solid State Chem.*, 1993, **102**, 4.
- 15 R. H. Jones, J. M. Thomas, Q. Huo, R. Xu, M. B. Hursthouse and J. Chen, *J. Chem. Soc., Chem. Commun.*, 1991, 1520.
- 16 S. Oliver, A. Kuperman, N. Coombs, A. Lough and G. A. Ozin, *Nature (London)*, 1995, **378**, 47.
- 17 R. Kniep, *Angew. Chem., Int. Ed. Engl.*, 1986, **25**, 525.
- 18 J. S. Beck, J. C. Vartuli, W. J. Roth, M. E. Leonowicz, C. T. Kresge, K. D. Schmitt, C. T.-W. Chu, D. H. Olson, E. W. Sheppard, S. B. McCullen, J. B. Higgins and J. L. Schlenker, *J. Am. Chem. Soc.*, 1992, **114**, 10834.
- 19 Q. Huo, D. J. Margolese, U. Ciesla, P. Feng, T. E. Gier, P. Sieger, R. Leon, P. M. Petroff, F. Schuth and G. D. Stucky, *Nature (London)*, 1994, **368**, 317.
- 20 Y. Xu, X. Jiang, X. Meng and R. Xu, *Acta Petrol. Sin.*, 1987, **3**, 101.
- 21 R. A. van Nordstrand, D. S. Santilli and S. I. Zones, *ACS Symp. Ser.*, 1988, **368**, 236.
- 22 M. E. Davis, P. E. Hathaway, C. Montes and J. M. Gares, *Stud. Surf. Sci. Catal.*, 1989, **49**, 199.
- 23 A. Stein, B. Wehrle and M. Jansen, *Zeolites*, 1993, **13**, 291.
- 24 M. E. Davis, C. Montes, P. E. Hathaway, J. P. Arhancet, D. L. Hasha and J. Garces, *J. Am. Chem. Soc.*, 1989, **111**, 3919.
- 25 L. Maistran, Z. Gabelica, E. G. Derouane, E. T. C. Vogt and J. van Oene, *Zeolites*, 1991, **11**, 583.
- 26 K. Nakashiro, Y. Ono, S. Nakata and Y. Moyimura, *Zeolites*, 1993, **13**, 561.
- 27 N. J. Tapp, N. B. Milestone and D. M. Bibby, *Zeolites*, 1988, **8**, 183.
- 28 Q. Shen, *¹³C NMR Spectroscopy*, Peking University Press, Beijing, 1988.
- 29 Q. Gao, J. Chen, S. Li and R. Xu, *J. Microporous Mater.*, 1996, in the press.
- 30 Q. Gao, S. Li and R. Xu, *J. Chem. Soc., Chem. Commun.*, 1994, 1465.
- 31 Q. Huo, R. Xu, S. Li, Z. Ma, J. M. Thomas, R. H. Jones and A. M. Chippindale, *J. Chem. Soc., Chem. Commun.*, 1992, 875.
- 32 R. H. Jones, J. M. Thomas, J. Chen, R. Xu, Q. Huo, S. Li, Z. Ma and A. M. Chippindale, *J. Solid State Chem.*, 1993, **102**, 204.
- 33 S. B. McCullen, P. T. Reischman and D. H. Olson, *Zeolites*, 1993, **13**, 640.
- 34 P. E. Jr. Eberly, *J. Phys. Chem.*, 1963, **67**, 2404.
- 35 J. A. Martens, E. Feijen, J. L. Lievens, P. J. Crobet and P. A. Jacobs, *J. Phys. Chem.*, 1991, **95**, 10025.
- 36 C. A. Fyfe, H. Grondey, K. T. Muller, K. C. Wong-Moon and T. Morkus, *J. Am. Chem. Soc.*, 1992, **114**, 5876.
- 37 Y. Wu, D. Lewis, J. S. Frye, A. Palmer and R. A. Wind, *J. Magn. Reson.*, 1992, **100**, 425.

Received 17th April 1996; Paper 6/02681H